

Targeting Carbonic Anhydrases with Fluorescent BODIPY-Labelled Sulfonamides

Philip A. Waghorn,^{*[a]} Michael W. Jones,^[a] Alan McIntyre,^[b] Alessio Innocenti,^[c] Daniela Vullo,^[c] Adrian L. Harris,^[b] Claudiu T. Supuran,^[c] and Jonathan R. Dilworth^[a]

Keywords: Carbonic anhydrases / Sulfonamides / Fluorescence / BODIPY / Imaging agents

In the pursuit of dual-mode imaging agents of the tumour hypoxia markers carbonic anhydrases (CA) IX and XII, sulfonamides 4-(2-aminoethyl)benzenesulfonamide and 1,3,4-thiadiazole were functionalised with a 4,4-difluoro-4-borata-3a-azonia-4a-aza-*s*-indacene (BODIPY) dye to afford fluorescent aromatic sulfonamide conjugates as potential agents for simultaneous positron emission tomography and fluorescence imaging. Both compounds exhibited nanomolar po-

tency as inhibitors of four CA isoforms: the cytosolic CA I and II, and the transmembrane CA IX and XII. Cell uptake experiments with a CA IX positive and null cell line showed no uptake with the 1,3,4-thiadiazole species in either cell line, whilst the benzenesulfonamide species showed uniform internalisation in both cell lines that limited these compounds as selective imaging agents.

Introduction

Whilst fluorine-18 remains the radionuclide of choice in positron emission tomography (PET),^[1–3] new expedient methods for the ¹⁸F labelling of small molecules, peptides and antibodies that avoid challenging multistep carbon–fluorine bond formation remain to be found. To this end, alternative strategies that employ the facile formation of strong fluorine–metal bonds have been considered, with particular focus on the ¹⁸F labelling of boron, silicon and aluminium.^[1,4–9] Fluorine bonds to boron are some of the thermodynamically most stable covalent bonds known,^[10,11] which has driven the development of radiopharmaceuticals that contain B–F bonds, such as the ¹⁸F-labelled tetrafluoroborate for thyroid imaging.^[12–14] Several examples of functionalised ¹⁸F-labelled aryl boronic esters have been established as radiolabelling strategies for labelling biomolecules or bifunctional linkers.^[15] These include the labelling of folic acid for folate receptor imaging,^[13] maleimide derivatives for conjugation to cysteine-containing peptides for imaging integrins^[1] and azide precursors for “click” chemistry assemblies.^[1]

A limitation of PET imaging, however, can be its low spatial resolution (1–2 mm). This can be resolved by a combination with a second imaging technique such as fluores-

cence, which offers much higher spatial and temporal resolution, thereby allowing a comprehensive picture of the bio-distribution of the imaging agent to be produced.^[16,17] Such dual-mode imaging capabilities are commonly achieved through the combination of the two imaging agents separately,^[18–20] whilst in principle a single agent that provides both fluorescent and radioimaging potential would allow for simpler syntheses and reduced modification of the targeting vector.

Recently, interest has focussed on the B–F-containing 4,4-difluoro-4-borata-3a-azonia-4a-aza-*s*-indacene (BODIPY) dyes, which not only provide high photochemical stability, high absorption coefficients and large fluorescence quantum yields,^[21,22] but also a potential radio-fluorine labelling site. Initially work with radiolabelling was achieved through an ¹⁸F-labelled boronic ester coupled to a BODIPY derivative, thus offering the potential for combined PET and fluorescence imaging with the same molecule.^[23] Recently, however, Gabbai et al.^[24] have made progress towards the direct labelling of neutral and cationic BODIPY species with fluoride, thereby achieving ¹⁸F labelling in water in a 61% radiochemical yield with a specific activity of >1.4 Ci μmol⁻¹, which has enabled the first in vivo and ex vivo dual-mode images of an ¹⁸F-labelled BODIPY species.^[25] Work by this group is currently underway to improve on the specific activity of labelling achieved with these agents.

One target of interest in oncology is the tumour-associated transmembrane carbonic anhydrases (CA).^[26] CAs are zinc metalloenzymes that catalyse the interconversion between CO₂ and HCO₃⁻, thereby maintaining a pH balance in blood plasma and transporting carbon dioxide out of tissue. Sixteen isoforms of CA have been identified to

[a] Chemistry Research Laboratory, University of Oxford, 12 Mansfield Road, Oxford, OX1 3TA, UK
Fax: +44-1865-285002

E-mail: philip.waghorn@oncology.ox.ac.uk

[b] Cancer Research UK Growth Factor Group, Weatherall Institute of Molecular Medicine, John Radcliffe Hospital, Oxford, OX3 9DS, UK

[c] Università degli Studi di Firenze, Laboratorio di Chimica Bioinorganica, Room 188, Via della Lastruccia 3, 50019 Sesto Fiorentino (Firenze), Italy

date;^[27] they are located in the cytosol, mitochondria and cellular membranes, or present as a secreted form (CA VI). Particular interest surrounds the transmembrane CA IX isozyme, which has been found to be overexpressed in certain cancer lines including renal,^[28,29] cervical squamous,^[30] breast,^[31,32] colorectal,^[33,34] bladder^[35] and non-small-cell lung carcinoma.^[36] A strong association between CA IX expression and intratumoural hypoxia has also been demonstrated^[37] as a result of strong transcriptional activation of the CA IX gene by HIF-1 α .^[28] Studies on non-small-cell lung carcinomas have shown CA IX association with proteins involved in angiogenesis, apoptosis inhibition and cell-cell adhesion disruption, which suggests a strong relationship of this enzyme with a poor clinical outcome.^[38] Similar interest surrounds CA XII, a second transmembrane tumour-associated CA isozyme with an extracellular active site that has been identified in renal cell carcinoma.^[39] As a result, interest lies in the development of CA inhibitors as an approach to the treatment of cancers in which CA IX/XII is overexpressed. Recent work has shown that the inhibition of CA IX has a strong anticancer effect with growth delay of both primary tumours and metastases.^[40,41] As such, the inhibition of these tumour-associated CA isozymes could represent a novel therapeutic approach for the management of hypoxic tumours that overexpress these proteins.

Primary aromatic and heterocyclic sulfonamides are potent inhibitors of CAs. Despite a nonspecific action against different CA isozymes, structural modifications can be introduced to induce selectivity toward specific isoforms.^[38,42–44] For instance, fluorescent imaging of CA IX by the incorporation of a fluorescein group {[4-sulfamoylphenylethyl]thioureido]fluorescein (FTES); Figure 1a} has been achieved, with enzyme-modelling studies suggesting that the combination of increased bulk and hydrogen-bonding interactions between a guanidine residue specific to CA IX and the carbonyl oxygen atom of the fluorescein tail of the inhibitor accounts for the much increased affinity of FTES for CA IX over the ubiquitous CA II enzyme.^[45]

Recently, Sando et al. have investigated 8-(4-aminosulfonylphenyl)-BODIPY (Figure 1b) as a selective inhibitor dye conjugate for “turn-on” fluorescence sensing of CAs.^[46] In the presence of CA, a twofold enhancement in fluorescence intensity was observed as a result of the increased steric constraints imposed by the active site of the enzyme, which acts to reduce the nonradiative mechanisms of fluorescent decay. Similarly, Gay et al.^[47] have previously investigated an acetazolamide-functionalised BODIPY 556/558 dye (Figure 1c) for CA II binding of osteoclasts. Inhibition of bone resorption through reduced H⁺ release upon sulfonamide binding was confirmed by reduced fluorescence emission under competition studies with unlabelled sulfon-

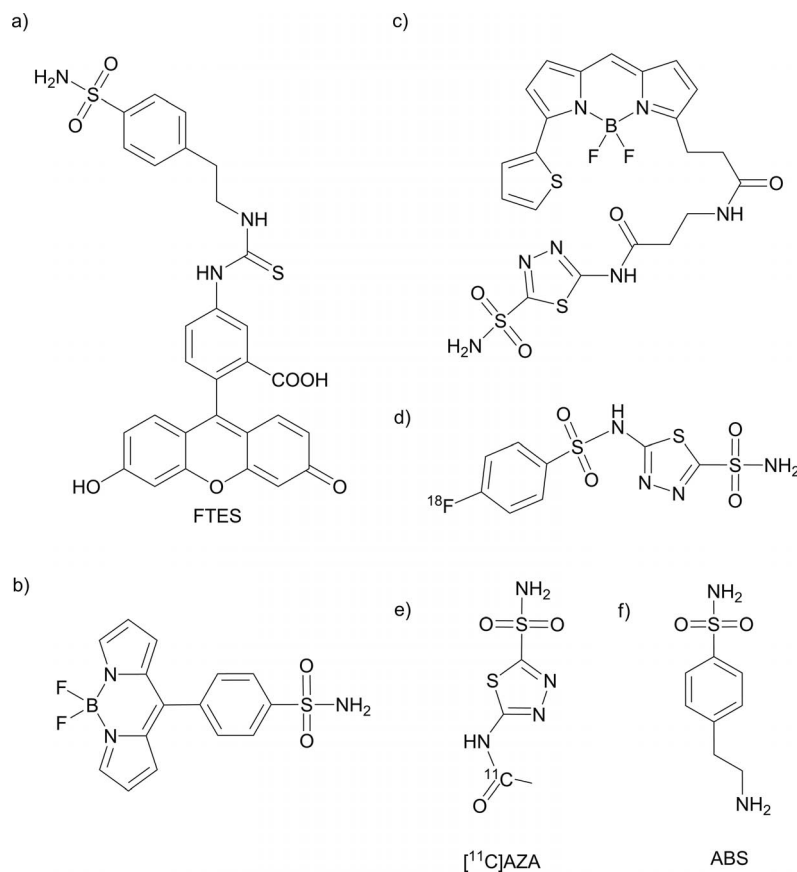


Figure 1. Structures of (a) [(4-sulfamoylphenylethyl)thioureido]fluorescein (FTES); (b) 8-(4-aminosulfonylphenyl)-BODIPY; (c) BODIPY 558/558 acetazolamide; (d) [¹⁸F]5-(*p*-fluorobenzenesulfonamido)-1,3,4-thiadiazole-2-sulfonamide; (e) acetazolamide (AZA); and (f) 4-(2-aminoethyl)benzenesulfonamide (ABS).

amide inhibitors. However, no data on the specific CA IX/XII inhibition was reported in either of these studies.

There are relatively few reports that involve the labelling of sulfonamides with radioisotopes for nuclear imaging. [^{18}F]5-(*p*-fluorobenzenesulfonamido)-1,3,4-thiadiazole-2-sulfonamide (Figure 1d) has been prepared by an aromatic nucleophilic substitution reaction of the nitro group precursor with radioactive fluoride and was shown to act as a nanomolar inhibitor of CA II and CA IV,^[48] and Le Bars et al.^[49] have prepared ^{11}C -labelled acetazolamide (AZA) (Figure 1e) to study lung CA inhibition.

Chelators such as ethylenediaminetetraacetic acid (EDTA) or diethylenetriaminepentaacetic acid (DTPA) have been conjugated to sulfonamides with retention of CA IX inhibition, thus enabling the binding of metal radioisotopes such as copper-64,^[50–52] although radiolabelling studies have not yet been carried out.

Given the present interest in ^{18}F -labelling of B–F bonds and the recent progress towards the direct ^{18}F labelling of BODIPY adducts in high specific activity, we describe here the synthesis and preliminary CA inhibition and fluorescence studies of arylsulfonamides functionalised with a BODIPY dye as analogues of the FTES dye. The identification of agents as specific CA IX/XII inhibitors will allow further modification of the BODIPY boron core, thus allowing individual ^{18}F radiolabelling strategies to be developed and optimised in parallel with current established methods.^[25] This paper describes our preliminary steps towards dual-mode imaging agents for targeted fluorescence and radioimaging of selective transmembrane CA expression.

Results and Discussion

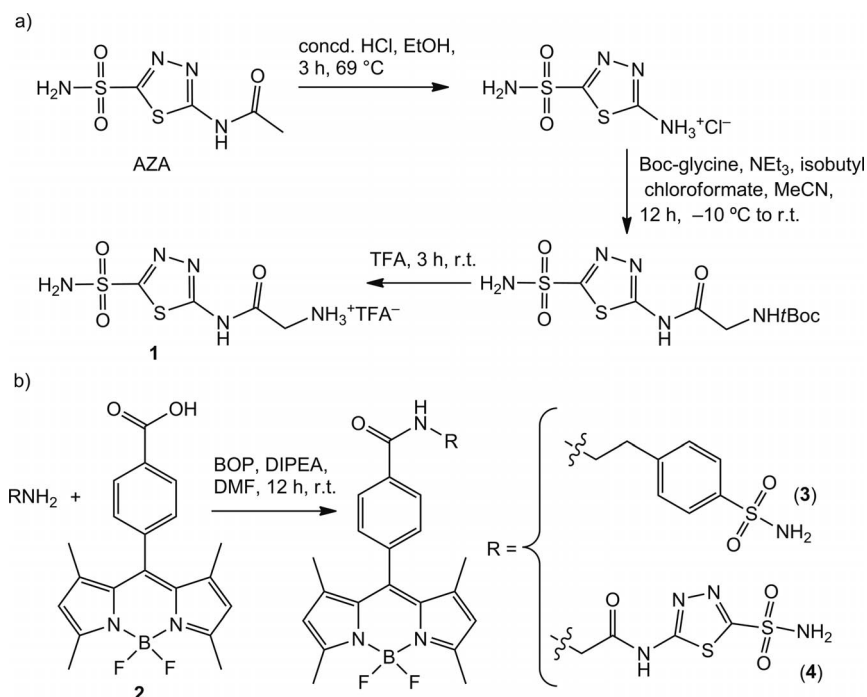
Synthesis and Chemical Properties

BODIPY conjugates of two well-known CA IX and XII inhibitors that incorporate the sulfonamide motif were investigated.

ABS (Figure 1f) is an efficient and specific CA IX and XII inhibitor but is less selective toward the widely distributed cytoplasmic CA II and the plasma-membrane-anchored CA IV.^[38,44] AZA is itself a nonspecific inhibitor of several CAs but has shown selectivity toward CA IX and CA XII with respect to CA II when structurally modified with fluorescein,^[53] DTPA^[50] and boroxalidones.^[54]

The target compounds were prepared by the (benzotriazol-1-yloxy)tris(dimethylamino)phosphonium hexafluorophosphate (BOP) mediated peptide coupling of ABS or AZA-NH₂ (**1**) to BODIPY-CO₂H (**2**) to afford the ABS-BODIPY (**3**) and AZA-BODIPY (**4**) conjugates in 81 and 73% yield, respectively (Scheme 1b). BODIPY-CO₂H (**2**) was prepared according to a literature procedure,^[55] whereas **1** was synthesised from AZA according to an adapted literature procedure, as shown in Scheme 1a.^[56]

Fluorescence quantum yields were measured for **3** and **4** in both methanol and a water/methanol (95:5) solution (Table 1). Addition of the sulfonamide groups caused some quenching of fluorescence with respect to the parent compound **2**, though the quantum yields remained high. Comparable quantum yields were obtained for measurements made in both H₂O and MeOH, with no quenching in H₂O, thereby suggesting their suitability for in vitro fluorescence imaging.



Scheme 1. (a) Synthesis of **1**. (b) Synthesis of **3** and **4**.

Table 1. Fluorescent quantum yield data for **2**, **3** and **4**.

BODIPY	λ_{abs} [nm]	λ_{em} [nm]	ϵ [$10^5 \text{ mol}^{-1} \text{ dm}^3 \text{ cm}^{-1}$]	Φ (MeOH) ^[a,b]	Φ (H ₂ O) ^[a,b]
2	500	509	0.98	0.46	0.44
3	499	511	0.83	0.39	0.36
4	499	511	0.87	0.39	0.35

[a] $\lambda_{\text{exc}} = 496 \text{ nm}$. [b] Referenced against fluorescein in 0.1 M NaOH, $\Phi = 0.95$,^[57] $\lambda_{\text{exc}} = 496 \text{ nm}$. All Φ values are corrected for changes in refractive index.

X-ray Crystallography

Red crystals of **3** and **4** were grown by slow infusion of diethyl ether or hexane into solutions of the respective compounds in THF (Figure 2), with the structures broadly similar to previously structurally characterised BODIPY derivatives.^[58,59]

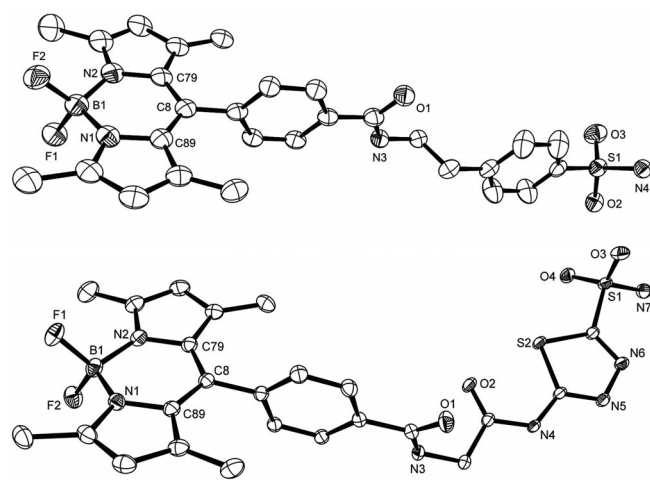


Figure 2. ORTEP representation of the structures of **3** (top) and **4** (bottom) with thermal ellipsoids at 30% probability. Minor disordered components and solvent molecules have been omitted for clarity.

The central six-membered ring in both structures lies coplanar with the adjacent five-membered rings to ensure a planar BODIPY framework with π -electron delocalisation over the indacene core, with the BF₂ unit perpendicular to this core. The dihedral angle between the phenyl group at the *meso* position and the BODIPY indacene skeleton is 85.88° for **3** and 82.88° for **4**, and it is indicative of the restriction that the methyl groups of the dipyrromethene frame impart on the free rotation of the phenyl substituents at the *meso* position. These interactions are integral to the reduced loss of energy from electronically excited states through non-irradiative molecular relaxation and hence the increased fluorescence quantum yield of this class of compounds.^[60] Selected bond lengths and angles for **3** and **4** are given in Table 2.

A number of C–H...F short-range interactions and S/C=O...H intermolecular hydrogen-bonding interactions are present in the packing of each structure. In the solid state of **3**, the molecules are aligned in pairs in a tail-to-tail arrangement as a result of short-range hydrogen-bonding in-

Table 2. Selected bond lengths [Å] and angles [°] for the X-ray structures of **3** and **4**.

	3	4	3	4	
B1–F1	1.399(4)	1.387(2)	S1–O3	–	1.442(3)
B1–F2	1.398(5)	1.406(3)	S1–O4	–	1.423(3)
B1–N1	1.549(6)	1.534(3)	S1–N7	–	1.600(3)
B1–N2	1.527(6)	1.543(3)	S1–O2	1.442(3)	–
N1–C89	1.403(5)	1.402(2)	S1–O3	1.423(3)	–
N2–C79	1.400(5)	1.401(2)	S1–N4	1.600(3)	–
C8–C89	1.391(5)	1.397(3)	N1–B1–N2	107.3(3)	107.3(3)
C8–C79	1.407(5)	1.404(2)	F1–B1–F2	108.0(3)	108.0(3)

teractions that exist between adjacent sulfonamide groups with bonding distances of 2.137 Å for N4–H42...O3* (Figure 3a).

Adjacent pairs are aligned in a head-to-tail formation by hydrogen-bonding interactions between the adjacent sulfonamide amine and amide carbonyl groups O1...H41–N4* (1.978 Å) (Figure 3a). These infinite chains are further held together through three short-range B–F...H–C bonding interactions (2.303–2.573 Å) (Figure 3b). Further hydrogen bonding is present between the amide nitrogen atom and solvent molecule (diethyl ether) oxygen atom (2.505 Å) (Figure 3a).

Compound **4** was co-crystallised with two THF molecules, and hydrogen bonding exists between the solvent THF oxygen atoms with the sulfonamide nitrogen atoms (1.935 Å) and the carboxyphenyl amide nitrogen atoms (2.044 Å). A third severely disordered THF molecule that was not hydrogen-bonded was unable to give a sensible model and hence removed by SQUEEZE.^[61–63] Hydrogen-bonding interactions are also present between the thiadiazole nitrogen atom and the amide nitrogen atom on adjacent molecules (2.008 Å) (Figure 3c). In **4** short-range interactions were observed between the B–F unit and the sulfonamide amine groups (2.022 Å) and between the B–F unit and the aromatic ring (2.573 Å) (Figure 3d).

In Vitro Studies of the BODIPY–Sulfonamide Conjugates

Preliminary in vitro uptake experiments were performed on a HeLa cell line to ascertain whether or not fluorescence emission could be observed. Complex **3** showed strong uniform distribution in the cytoplasm of the HeLa cell line after only 30 min of incubation, with no nuclear staining observed. No difference in uptake pattern was observed between experiments conducted at either 4 or 37 °C, thereby

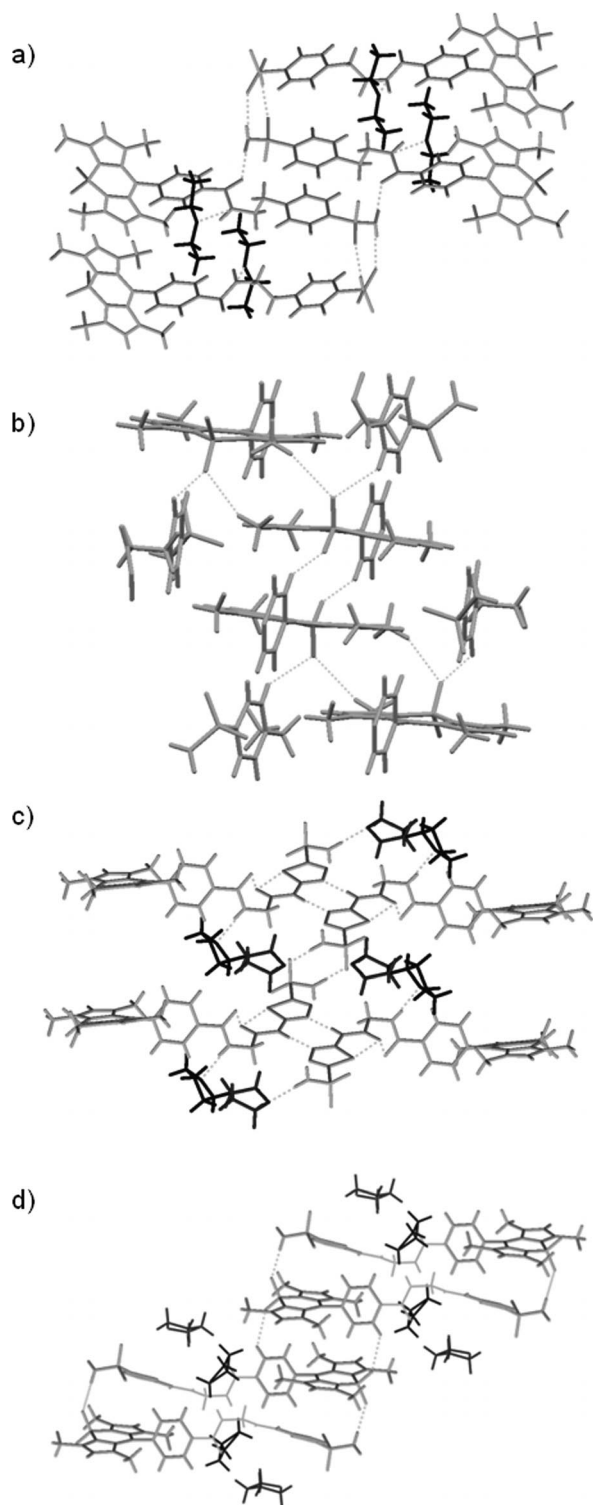


Figure 3. Packing diagrams depicting symmetry elements of $3 \cdot \text{Et}_2\text{O}$, showing (a) hydrogen-bonding interactions and (b) short-range interactions with the B–F unit (Et_2O omitted for clarity). Packing diagrams depicting symmetry elements of $4 \cdot 2\text{THF}$, showing (c) hydrogen-bonding interactions and (d) short-range interactions with The B–F unit.

suggesting that the mode of internalisation is by passive diffusion. Conversely, compound **4** showed no uptake in the HeLa cell line after 30 min of incubation.

To establish the effect and selectivity on cell uptake of the two conjugates in the presence of the CA IX enzyme, cell-uptake experiments were conducted on an HCT116 colon carcinoma cell line transfected to overexpresses the CA IX enzyme [HCT116 (CA9+)]. Control uptake experiments were performed on the HCT116 null CA IX empty vector cell line [HCT116 (EV)], with fluorescence-activated cell sorting (FACS) analysis performed on a fluorescently labelled CA IX antibody in parallel to confirm the presence or lack of CA IX expression in the two cell lines.

Cell uptake experiments were repeated with **3** and **4** over a 24 h incubation period and imaged by epifluorescence microscopy with the fluorescein–sulfonamide conjugate FTES run in parallel as a positive control. After 24 h, **4** showed no uptake either in the membrane or internalised in either cell line, whereas **3** showed uptake in both the CA IX positive and empty-vector cell lines (Figure 4). By comparison, the FTES standard stained only the positive control with no fluorescein fluorescence emission associated with the empty-vector cell line.

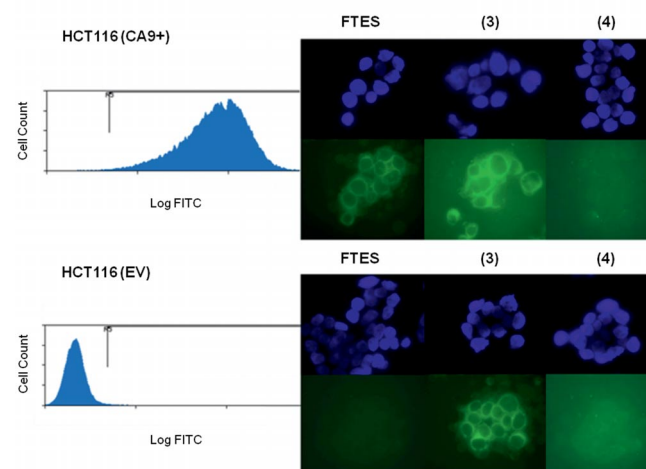


Figure 4. Epifluorescence uptake studies of FTES, **3** and **4** in HCT116 (CA9+) and HCT116 (EV) cell lines co-stained with 4',6-diamidino-2-phenylindole (DAPI; blue stain). FACS analysis using a fluorescein-isothiocyanite labelled CA IX antibody were conducted concomitantly as a second positive control of CA IX expression. Each field of view is 100 by 80 μm .

Whereas fluorescein is impermeable to the cell membrane and hence promotes the selective transmembrane CA IX binding, the BODIPY dye is internalised rapidly into cells^[64] by a process of diffusion, which, in the case of compound **3**, prevents significant interactions with the membrane-bound CA IX and hence an observed lack of specificity with uptake in both the CA IX positive and control empty-vector HCT116 cell lines. Conversely to this and to the work of Gay et al.,^[47] despite the strong cell uptake of both the BODIPY dye alone and AZA itself (as shown by Gay et al. through ^3H -labelling studies^[65,66]) their conjugate, **4**, showed no cellular uptake, which suggests that the thiadiazole group once conjugated makes this BODIPY de-

FULL PAPER

Table 3. Inhibition of CA isoforms human CA (hCA) I, II, IX and XII with sulfonamides **3** and **4** compared to the starting materials ABS and AZA and FTES. Errors in the range of ± 5 –10% of the reported value, from three different determinations.

Inhibitor	K_i^* [nM] hCA I ^[a]	hCA			Selectivity ratios			
		hCA II ^[a]	hCA IX ^[b]	hCA XII ^[c]	hCA IX/hCA I	hCA IX/hCA II	hCA XII/hCA I	hCA XII/hCA II
3	301	31	63	78	4.8	0.5	3.9	0.4
4	90	67	70	89	1.3	1.0	1.0	0.8
ABS ^[38,44]	21000	160	33	3.2	636.4	4.9	6563	50
AZA ^[42]	250	12	25	5.7	10.0	0.5	43.9	2.1
FTES ^[42]	1300	45	24	5.0	54.2	1.9	260	9.0

[a] Human (cloned) isozymes. [b] Catalytic domain of the human, cloned isozyme. [c] Catalytic domain of the human recombinant isozyme, CO₂ hydrase assay method.

rivative cell impermeable. Whereas cell impermeability in the empty-vector cell line is preferable to ensure enhanced contrast, unlike the FTES species, no CA IX binding was observed. Estimates of the partition coefficient ($\log P$) values of **3** and **4** were made to attempt to ascertain an explanation for the lack of cell permeability of compound **4**. Comparable results were obtained for both **3** and **4** with $\log P$ values of 1.57 ± 0.15 and 1.43 ± 0.11 , respectively. These results are in keeping with the HPLC retention times and suggest that both species are lipophilic with complex **4** showing an increased hydrophilicity, though this is not sufficient to explain the observed differences in cell permeability of these two complexes, which remains uncertain.

To attempt to understand the lack of CA IX binding by **4** under in vitro studies, the binding affinities of the BODIPY sulfonamides **3** and **4** compared with FTES were carried out with the CA isoforms in isolation. Inhibition data against four CA isozymes (CA I, CA II, CA IX and CA XII) was measured, and the results are given in Table 3 together with the data for the parent sulfonamides AZA and ABS. The data from the enzyme inhibition suggests that the binding affinities of the BODIPY derivatives to the transmembrane CA IX and XII isozymes are significantly weaker than those of FTES and the AZA and ABS groups alone, and the selectivity for CA IX and CA XII with respect to the ubiquitous CA enzymes CA I and CA II is poor by comparison.

Compound **4** binds to all four CA enzymes investigated with uniform affinity with a threefold and eighteenfold weaker binding affinity toward the CA IX enzyme and CA XII enzyme, respectively, relative to that of FTES. Compound **3** shows a weak binding affinity for CA I with a selectivity ratio of 4.8 for CA IX/CA I and 3.9 for CA XII/CA I, although its binding affinity for the transmembrane CAs is less than half that of the affinity for the ubiquitous CA II isoform. The comparable sizes of the BODIPY dyes with the fluorescein compound would suggest favourable CA IX selectivity for the BODIPY conjugates as a result of the increased size of the CA IX cavity relative to the ubiquitous CA II isozyme.^[43] However, the lack of secondary hydrogen-binding interactions between these BODIPY-functionalised sulfonamides and the CA IX enzyme as observed for the FTES derivative hinders selective inhibition, thus leading to weaker binding affinity and poor CA selectivity and the apparent lack of fluorescence emission for **4** in the HCT116 (CA9+) cell line.

Conclusion

Despite the favourable fluorescence properties and recent routes towards ¹⁸F radiolabelling of BODIPY dyes, both BODIPY–sulfonamide conjugates lack selectivity for the transmembrane CA IX and CA XII isozymes as measured by the stopped-flow binding-affinity assay. The comparable size of the BODIPY dyes with the fluorescein species should parallel CA IX selectivity over CA II binding, but – whereas the fluorescein adduct provides secondary binding interaction with the CA IX enzyme active site – the BODIPY indacene core does not provide similar hydrogen-bonding interactions and therefore lacks enzyme selectivity. In the case of **3**, uptake is dominated by the BODIPY dye entity, and – whereas with **4** cellular uptake in the control samples was minimised – the weak CA IX binding affinity resulted in similarly negligible CA IX interaction in the positive cell line.

Future modifications to make the BODIPY dye charged and cell-impermeable and the use of a greater library of sulfonamides may yet yield selective contrast agents for dual-mode PET and fluorescence imaging based on the BODIPY motif.

Experimental Section

General: All reactions were carried out in oven-dried glassware under nitrogen. Nitrogen gas was dried by passage through silica gel. All solvents were dried according to standard procedures. All reagents were purchased from Aldrich and used without further purification. Column chromatography was performed on silica gel 60M (mesh 230–400) from Macherey–Nagel. ¹H NMR spectra were recorded with a Varian Mercury VX300 (300 MHz) spectrometer at 298 K and referenced to residual nondeuterated solvent peaks. Chemical shifts are quoted in ppm. Coupling constants (J) are measured to the nearest 0.1 Hz and are presented as observed. ¹³C NMR spectra were recorded with a Varian Mercury VX300 (75.5 MHz) spectrometer at 298 K and were referenced to the solvent peak.^[67] ¹⁹F NMR spectra were recorded with a Varian Mercury VX300 (282 MHz) at 298 K and were referenced to a fluoro-benzene spike ($\delta = -113.15$ ppm). NMR spectra were processed by using MestReC software. Mass spectrometry was performed with a Bruker Micromass LCT time-of-flight mass spectrometer under electrospray ionisation (ESI-MS) conditions. Accurate masses are reported to four decimal places by using tetraoctylammonium bromide (466.5352 Da) as an internal reference. Values are reported as a ratio of mass to charge in Daltons. HPLC characterisation (analytical HPLC) of compounds was performed with a Waters C-

18 column (4.6 × 250 mm) and UV/Vis detection at $\lambda_{\text{obs}} = 254$ and 410 nm with a 1.0 mL min⁻¹ gradient elution method (solvent A: acetonitrile with 0.1% TFA, v/v; solvent B: water with 0.1% TFA, v/v): start with 5% of A, gradient over 23 min to reach 95% of A, hold at 25 min at 95% of A, reverse gradient for 27 min to reach 5% A, then hold for 30 min at 5% A. Elemental analyses were performed either by the microanalysis service in the Inorganic Chemistry Department at the University of Oxford or by Mr. S. Boyer at the London Metropolitan University for electronic absorption spectroscopy. UV/Vis spectroscopy was performed with a Perkin–Elmer Lambda 19 spectrometer that was running UV Winlab software. Spectra were measured by using 1.00 cm quartz cuvettes. Fluorescence spectra were recorded in 1.00 cm quartz cuvettes with a Hitachi F-4500 fluorescence spectrometer that was running FL Solutions software. Relative quantum yields were determined by comparison to fluorescein in 0.1 M NaOH ($\Phi_{\text{R}} = 0.95$ at 496 nm) by using the formula: $\Phi_{\text{S}} = \Phi_{\text{R}} \cdot (D_{\text{S}}/D_{\text{R}}) \cdot (A_{\text{R}}/A_{\text{S}}) \cdot (I_{\text{R}}/I_{\text{S}}) \cdot (\eta_{\text{S}}/\eta_{\text{R}})^2$ in which the variable Φ is the relative quantum yield, D is the integrated area of the fluorescence emission peak, A is the absorption of the solutions at the excitation wavelength, I is the flux at the excitation wavelength used, and η is the solution refractive index. R and S subscripts refer to the reference and sample, respectively.

2-Oxo-2-(5-sulfamoyl-1,3,4-thiadiazol-2-ylamino)ethanaminium Trifluoroacetate (1)

(a) **5-Amino-1,3,4-thiadiazole-2-sulfonamide**:^[56] A mixture of acetazolamide (1.00 g, 4.50 mmol), concentrated HCl (2.00 mL) and ethanol (15.0 mL) was heated under reflux conditions for 3 h. The solvent was evaporated in vacuo to near dryness, and the remaining suspension was allowed to cool slowly to room temp. The solid was collected by filtration and dried in vacuo (528 mg, 2.93 mmol, 65%). ¹H NMR (300 MHz, [D₆]DMSO, 25 °C): $\delta = 8.05$ (s, 2 H, SO₂NH₂), 7.79 (s, 2 H, thiadiazole-NH₂) ppm. ESI-MS: calcd. for C₂H₄N₄O₂S₂ [M – H]⁻ 178.9776; found 178.9758.

(b) **tert-Butyl [2-Oxo-(5-sulfamoyl-1,3,4-thiadiazol-2-ylamino)ethyl]carbamate**: *tert*-Butoxycarbonyl (Boc) glycine (87.5 mg, 0.500 mmol) and NEt₃ (70 μ L, 0.500 mmol) in MeCN (1.50 mL) was cooled to –10 °C, and isobutyl chloroformate (65.3 μ L, 0.500 mmol) was added with stirring. After 20 min at –10 °C, a shaken suspension of 5-amino-1,3,4-thiadiazole-2-sulfonamide (90.0 mg, 0.500 mmol) in MeCN (1.50 mL) that contained NEt₃ (70.0 μ L, 0.500 mmol) was added. The mixture was stirred at room temp. overnight and the solvent evaporated. The solid was recrystallised from a water/EtOH mixture to give a crystalline white solid (102 mg, 0.300 mmol, 61%). ¹H NMR (300 MHz, [D₆]DMSO, 25 °C): $\delta = 13.09$ (s, 1 H, CONH-thiadiazole), 8.28 (s, 2 H, SO₂NH₂), 7.31 (t, $J = 6.3$ Hz, 1 H, BocNHCH₂CONH), 3.87 (d, $J = 6.1$ Hz, 2 H, BocNHCH₂CONH), 1.32 (s, 9 H, *Boc*NH) ppm. ESI-MS: calcd. for C₉H₁₅N₅O₅S₂ [M – H]⁻ 336.0515; found 336.0524.

(c) **2-Oxo-2-(5-sulfamoyl-1,3,4-thiadiazol-2-ylamino)ethanaminium Trifluoroacetate**: *tert*-Butyl [2-oxo-(5-sulfamoyl-1,3,4-thiadiazol-2-ylamino)ethyl]carbamate (122 mg, 0.362 mmol) was added to TFA (5.00 mL) at room temp. and stirred for 3 h. The TFA was evaporated under reduced pressure and the residue dried in vacuo (110 mg, 0.313 mmol, 87%). ¹H NMR (300 MHz, [D₆]DMSO, 25 °C): $\delta = 13.46$ (br. s, 1 H, CONH-thiadiazole), 8.38 (s, 2 H, SO₂NH₂), 5.24 (m, 3 H, NH₃CH₂CONH), 3.96 (m, 2 H, NH₃CH₂CONH) ppm. ¹³C NMR (75.5 MHz, [D₆]DMSO, 25 °C): $\delta = 167.5, 165.7, 164.7, 161.5, 116.5, 41.8$ ppm. ESI-MS: calcd. for C₄H₈N₅O₃S₂ [M – CF₃CO₂]⁺ 238.0063; found 238.0081.

4,4-Difluoro-8-(4'-carboxyphenyl)-1,3,5,7-tetramethyl-4-bora-3a,4a-diaza-s-indacene (2): Complex **2** was synthesised according to a literature procedure.^[55] Pyrrole (1.35 mL, 19.4 mmol) and 4-formylbenzoic acid (1.30 g, 8.63 mmol) were dissolved in CH₂Cl₂ (1.00 L) under nitrogen. Two drops of TFA were added, and the solution was stirred at room temp. for 1 h. 2,3-Dichloro-5,6-dicyano-1,4-benzoquinone (DDQ; 1.96 g, 8.63 mmol) was added to CH₂Cl₂ (20.0 mL), and the solution was stirred for 1 h, after which NEt₃ (20.0 mL) and BF₃·OEt₂ (20.0 mL) were added dropwise. The reaction mixture was stirred at room temp. for 2 h before being quenched by the addition of water (500 mL) and extracted with CH₂Cl₂ (3 × 200 mL). The combined organic extracts were dried with anhydrous MgSO₄, filtered and concentrated under reduced pressure. The crude oil was purified by silica gel chromatography (0–8% MeOH in CH₂Cl₂) to yield a red solid after recrystallisation from THF/hexanes (701 mg, 1.90 mmol, 22%). ¹H NMR (300 MHz, [D₆]DMSO, 25 °C): $\delta = 13.25$ (br. s, 1 H, COOH), 8.10 (d, $J = 7.9$ Hz, 2 H, ArH), 7.53 (d, $J = 8.2$ Hz, 2 H, ArH), 6.20 [s, 2 H, NC(CH₃)CHC(CH₃)], 2.46 [s, 2 × 3 H, NC(CH₃)CHC(CH₃)], 1.33 [s, 2 × 3 H, NC(CH₃)CHC(CH₃)] ppm. ¹⁹F NMR (282 MHz, [D₆]DMSO, 25 °C): $\delta = -143.7$ [q, $J(\text{B},\text{F}1) = 34$ Hz, 2 F, BF] ppm. ¹³C NMR (75.5 MHz, [D₆]DMSO, 25 °C): $\delta = 167.3, 155.7, 150.2, 143.1, 138.8, 135.5, 131.9, 130.6, 128.8, 122.0, 14.7, 14.5$ ppm. ESI-MS: calcd. for C₂₀H₁₈BF₂N₂O₂ [M – H]⁻ 367.1435; found 367.1442. HPLC: $t_{\text{R}} = 14.72$ min.

General Amide Coupling Procedure: *N,N*-Diisopropylethylamine (DIPEA; 1.50 equiv.) was added to a stirred solution of BODIPY–CO₂H (**2**) (1.00 equiv.) in DMF (5.00 mL) and the solution was cooled to 0 °C in an ice bath. BOP (1.50 equiv.) was added, and the solution was stirred at 0 °C for 30 min. Amine (1.20 equiv.) was added, and the solution was warmed to room temperature and stirred for 12 h. The DMF was removed under reduced pressure. The crude product was dissolved in CHCl₃ (25.0 mL) and washed sequentially with 1 M HCl (20.0 mL), saturated NaHCO₃ (aq.) (100 mL), water (100 mL), brine (100 mL) and was dried with anhydrous MgSO₄. The CHCl₃ was removed under reduced pressure, and the crude residue was purified by silica gel chromatography.

4,4-Difluoro-8-[(4-sulfamoylphenethyl)benzamido]-1,3,5,7-tetramethyl-4-bora-3a,4a-diaza-s-indacene (3): Compound **3** was synthesised by employing the general amide coupling procedure with BOP (180 mg, 0.407 mmol), **2** (100 mg, 0.272 mmol), DIPEA (52.6 mg, 70.9 μ L, 0.407 mmol) and ABS (65.4 mg, 0.326 mmol). Flash chromatography of the residue by using an elution gradient of 0–5% MeOH in CHCl₃ afforded the title product as a red solid (121 mg, 2.20 mmol, 81%). ¹H NMR (300 MHz, [D₆]DMSO, 25 °C): $\delta = 8.78$ (t, $J = 5.5$ Hz, 1 H, CONH), 7.99 (d, $J = 8.2$ Hz, 2 H, ArH), 7.75 (d, $J = 8.3$ Hz, 2 H, ArH), 7.48 (d, $J = 8.3$ Hz, 2 H, ArH), 7.44 (d, $J = 8.4$ Hz, 2 H, ArH), 7.30 (s, 2 H, SO₂NH₂), 6.17 [s, 2 H, NC(CH₃)CHC(CH₃)], 3.53 (m, 2 H, NHCH₂CH₂), 2.94 (t, $J = 7.3$ Hz, 2 H, NHCH₂CH₂), 2.44 [s, 2 × 3 H, NC(CH₃)CHC(CH₃)], 1.32 [s, 2 × 3 H, NC(CH₃)CHC(CH₃)] ppm. ¹³C NMR (75.5 MHz, [D₆]DMSO, 25 °C): $\delta = 166.0, 155.6, 144.2, 143.1, 142.5, 141.5, 137.2, 135.4, 130.9, 129.6, 128.5, 128.5, 126.2, 122.0, 41.0, 35.2, 14.7, 14.6$ ppm. ¹⁹F NMR (282 MHz, [D₆]DMSO, 25 °C): $\delta = -143.7$ [q, $J(\text{B},\text{F}1) = 34$ Hz, 2 F, BF] ppm. ESI-MS: calcd. for C₂₈H₂₉BF₂NaN₄O₃S [M + Na]⁺ 573.1919; found 573.1915. HPLC: $t_{\text{R}} = 13.06$ min. C₂₈H₂₉BF₂N₄O₃S (550.20): calcd. C 61.1, H 5.3, N 10.2; found C 60.8, H 5.2, N 10.0.

4,4-Difluoro-8-[2-oxo-2-(5-sulfamoyl-1,3,4-thiadiazol-2-ylamino)ethyl]benzamido-1,3,5,7-tetramethyl-4-bora-3a,4a-diaza-s-indacene (4): Compound **4** was synthesised by employing the general amide coupling procedure with BOP (180 mg, 0.407 mmol), **2** (100 mg,

FULL PAPER

0.272 mmol), DIPEA (52.6 mg, 70.9 μ L, 0.407 mmol) and **1** (115 mg, 0.326 mmol). Flash chromatography of the residue by using an elution gradient of 0–7% MeOH in CHCl_3 afforded the title product as a red solid (116 mg, 0.198 mmol, 73%). ^1H NMR (300 MHz, $[\text{D}_6]\text{DMSO}$, 25 $^\circ\text{C}$): δ = 13.28 (s, 1 H, CONH-thiadiazole), 9.23 (t, J = 5.6 Hz, 1 H, CONHCH₂), 8.35 (s, 2 H, SO₂NH₂), 8.07 (d, J = 8.3 Hz, 2 H, ArH), 7.53 (d, J = 8.3 Hz, 2 H, ArH), 6.19 [s, 2 H, NC(CH₃)CHC(CH₃)], 4.27 (d, J = 5.5 Hz, 2 H, CONHCH₂), 2.44 [s, 2 \times 3 H, NC(CH₃)CHC(CH₃)], 1.34 [s, 2 \times 3 H, NC(CH₃)CHC(CH₃)] ppm. ^{13}C NMR (75.5 MHz, $[\text{D}_6]\text{DMSO}$, 25 $^\circ\text{C}$): δ = 170.0, 166.9, 165.3, 161.8, 155.9, 143.3, 141.7, 137.9, 134.8, 131.1, 128.9, 128.4, 122.1, 43.5, 14.9, 14.7 ppm. ^{19}F NMR (282 MHz, $[\text{D}_6]\text{DMSO}$, 25 $^\circ\text{C}$): δ = –143.7 [q, $J(\text{B},\text{F})$ = 34 Hz, 2 F, BF] ppm. ESI-MS: calcd. for $\text{C}_{24}\text{H}_{24}\text{BF}_2\text{NaN}_7\text{O}_4\text{S}_2$ [M + Na]⁺ 610.1290; found 610.1298. HPLC: t_{R} = 11.93 min. $\text{C}_{24}\text{H}_{24}\text{BF}_2\text{N}_7\text{O}_4\text{S}_2$ (587.14): calcd. C 49.1, H 4.1, N 16.7; found C 48.9, H 4.0, N 16.7.

X-ray Structures: Single-crystal X-ray diffraction data were obtained for compounds **3** and **4**. In each case, a typical crystal was mounted by using the oil drop technique in perfluoropolyether oil at 150(2) K with a Cryostream N₂ open-flow cooling device.^[68] Diffraction data were collected by using graphite-monochromated Mo- K_α radiation (λ = 0.71073 Å) with a Nonius Kappa CCD diffractometer. For all data collections, series of ω scans were performed in such a way as to collect a complete data set to a maximum resolution of 0.77 Å. Data reduction including unit-cell refinement and interframe scaling was carried out with DENZO-SMN/SCALEPACK.^[69] Intensity data were processed and corrected for absorption effects by the multiscan method, based on

repeat measurements of identical and Laue equivalent reflections. Structure solution was carried out by using direct methods with the programs SIR92^[70] within the CRYSTALS software suite.^[71] In general, coordinates and anisotropic displacement parameters of all non-hydrogen atoms were refined freely except where disorder necessitated the use of “same-distance restraints” together with thermal similarity and vibrational restraints to maintain sensible geometry/displacement parameters. Hydrogen atoms were generally visible in the difference map and refined with soft restraints prior to inclusion in the final refinement by using a riding model.^[62] In the case of compound **4**, the difference Fourier map indicated the presence of diffuse electron density believed to be a molecule of disordered THF. PLATON/SQUEEZE^[61–63] was used and left a void from which the electron density was removed. CCDC-871337 (**3**) and -871338 (**4**) contain the supplementary crystallographic data for this paper. These data can be obtained free of charge from The Cambridge Crystallographic Data Centre via www.ccdc.cam.ac.uk/data_request/cif. Table 4 offers a summary of the crystal and refinement data for the X-ray structures.

Fluorescence Microscopy: HeLa cells and HCT116 cells were provided by Professor Adrian Harris, Weatherall Institute for Molecular Medicine, University of Oxford. Cells were seeded as monolayers in T75 tissue culture flasks, and cultured in Dulbecco’s modified Eagle medium (DMEM) supplemented with 10% foetal bovine serum, L-glutamine, penicillin and streptomycin. Cells were maintained at 37 $^\circ\text{C}$ in a 5% CO₂ humidified atmosphere and grown to approximately 85% confluence before being split by using 2.5% trypsin. For microscopy, cells were seeded onto chambered coverglass slides and incubated for 12 h to ensure adhesion. BODIPY

Table 4. Crystallographic data for compounds **3** and **4**.

	3	4
Empirical formula	$\text{C}_{28}\text{H}_{29}\text{BF}_2\text{N}_4\text{O}_3\text{S}\cdot 0.85\text{C}_4\text{H}_{10}\text{O}$	$\text{C}_{24}\text{H}_{24}\text{O}_4\text{BF}_2\text{N}_7\text{S}_2\cdot 2\text{THF}$
M_r	613.76	731.65
Temperature [K]	150	150
λ [Å]	0.71073	0.71073
Crystal system	monoclinic	triclinic
Space group	$C2/c$	$P\bar{1}$
a [Å]	14.9330(3)	9.23680(10)
b [Å]	25.7615(7)	12.6383(10)
c [Å]	17.3381(5)	12.3105(10)
α [°]	90	71.4912(4)
β [°]	105.1383(11)	86.8518(4)
γ [°]	90	86.8556(3)
V [Å ³]	6438.4(3)	1904.21(3)
Z	8	2
$D_{\text{calcd.}}$ [g cm ⁻³]	1.27	1.28
μ [mm ⁻¹]	0.153	0.199
$F(000)$	2591.0	768
Size [mm]	0.14 \times 0.19 \times 0.36	0.20 \times 0.38 \times 0.40
Crystal description	orange block	orange block
θ range collected [°]	5.0 $\leq \theta \leq$ 27.5	5.0 $\leq \theta \leq$ 27.5
Index ranges	–19 $\leq h \leq$ 19 –32 $\leq k \leq$ 33 –22 $\leq l \leq$ 22	–11 $\leq h \leq$ 12 –17 $\leq k \leq$ 18 0 $\leq l \leq$ 25
Reflections measured	37242	49579
Unique reflections	13161	8645
R_{int}	0.047	0.015
Reflections observed [$I > 3\sigma(I)$]	7036	8644
Transmission coefficients (min., max.)	0.89, 0.98	0.88, 0.96
Refined parameters	474	451
R or $R1$ (reflections observed)	$R = 0.117$	$R = 0.056$
wR or $R2$ (all data)	$wR = 0.253$	$wR = 0.096$
GoF	0.95	1.03
Residual electron (min., max.) [e Å ⁻³]	–0.67, 0.86	–0.50, 0.65

complexes were prepared as 10 mM solution in DMSO and diluted to 10 μ M with DMEM, and incubated with the cells at 37 °C. After 30 min or 24 h, the BODIPY solution was discarded, and the cells were washed with fresh DMEM medium before imaging. BODIPY complexes were imaged by laser-scanning confocal microscopy with a Zeiss LSM 510 META microscope irradiating at 488 nm, and emissions were filtered between 505 and 535 nm and with an Axiovert 135 inverted microscope (Zeiss, USA) visualised by using Axiovision software (Zeiss, USA) irradiating at 488 nm with emissions filtered above 500 nm.

Measurement of Partition Coefficient (log P): A solution (1 μ M) of each compound in 1-octanol was kept at 60 °C for 1 h. A UV spectrum was then recorded, and the value of absorbance at the maximum was measured (A_0). Equal volumes of organic solution and phosphate buffer (0.1 M, pH = 7.4) were vortexed (2500 rpm) for 1 min. The UV spectrum of the organic layer was determined after 30 min (A_x). The partition coefficient (log P) was calculated according to the relationship $P = A_x/(A_0 - A_x)$. A solution of *n*-octanol saturated with water was used as the blank.

FACS Analysis: Cells were detached and re-suspended on ice in phosphate buffer solution (PBS; 100 μ L), at a concentration of 2×10^6 cells per mL. Fluorescein isothiocyanate (FITC) labelled CA IX antibody (10 μ L, R&D systems, USA) was added and incubated at 4 °C for 1 h. Cells were washed with PBS and resuspended in PBS (500 μ L). Samples were analysed by flow cytometry with a FACSCalibur flow cytometer (BD Biosciences, USA) and CellQuest software (BD Biosciences, USA).

CA Inhibition: Binding affinities were measured with isolated CA enzymes. An Applied Photophysics stopped-flow instrument was used for the assay of the CA-catalysed CO₂ hydration activity. Phenol red (0.2 mM) was used as an indicator, working at the absorbance maximum of 557 nm, with *N*-(2-hydroxyethyl)piperazine-*N'*-ethanesulfonic acid (10 mM, pH = 7.5) used as buffer, and Na₂SO₄ (0.1 M) used to maintain constant ionic strength, all at 25 °C. The CA-catalysed CO₂ hydration reaction was monitored over 10–100 s (the uncatalysed reaction needed around 60–100 s under assay conditions, whereas the catalysed reactions required between 6 and 10 s). Each inhibitor was tested over the concentration range of 0.01 nM to 100 μ M. Stock solutions of inhibitor (1 mM) were prepared in distilled, deionised water with 10–20% (v/v) DMSO (which is not inhibitory at these concentrations). These stock solutions were diluted up to 0.01 nM with distilled, deionised water. Inhibitor and enzyme solutions were preincubated together at room temp. for 15 min prior to assay, which facilitated the formation of the enzyme–inhibitor complex. The inhibition constants and catalytic activity (in the absence of inhibitor) of these enzymes were calculated and represent the mean from three separate experiments. Enzyme concentrations in the assay system were 14 nM for hCA I, 10.5 nM for hCA II, 8.5 and 14.6 nM for hCA IX. The collected data from the stopped-flow assay was plotted as an inhibition percentage of the enzyme, against inhibitor concentrations, by using a sigmoidal dose–response curve. From this data the IC₅₀ (the concentration of BODIPY compound required to inhibit the turnover of CO₂ by the specific CA enzyme by 50%) was obtained by using Prism 4.0 software.^[72] The simplified Michaelis–Menton equation for steady state was then used to calculate the specific inhibitor constant K_i for the BODIPY compound with that particular CA enzyme.

Acknowledgments

P. A. W. and M. W. J. thank the Engineering and Physical Sciences Research Council (EPSRC) and the Medical Research Council

(MRC) for funding. A. M. and A. L. H. thank the Cancer Research UK and the EU Framework 7 Metoxia for funding. The authors also wish to thank Dr. Amber L. Thompson for helpful discussions.

- [1] G. E. Smith, H. L. Sladen, S. C. G. Biagini, P. J. Blower, *Dalton Trans.* **2011**, 40, 6196–6205.
- [2] S. Purser, P. R. Moore, S. Swallow, V. Gouverneur, *Chem. Soc. Rev.* **2008**, 37, 320–330.
- [3] P. W. Miller, N. J. Long, R. Vilar, A. D. Gee, *Angew. Chem.* **2008**, 120, 9136; *Angew. Chem. Int. Ed.* **2008**, 47, 8998–9033.
- [4] R. Schirrmacher, G. Bradmoeller, E. Schirrmacher, O. Thews, J. Tillmanns, T. Siessmeier, H. G. Bucholz, P. Bartenstein, B. Waengler, C. M. Niemeyer, K. Jurkschat, *Angew. Chem.* **2006**, 118, 6193; *Angew. Chem. Int. Ed.* **2006**, 45, 6047–6050.
- [5] E. Schirrmacher, B. Waengler, M. Cypriak, G. Bradtmöller, M. Schaefer, M. Eisenhut, K. Jurkschat, R. Schirrmacher, *Bioconjugate Chem.* **2007**, 18, 2085–2089.
- [6] L. Iovkova, B. Waengler, E. Schirrmacher, R. Schirrmacher, G. Quandt, B. Boening, M. Schuermann, K. Jurkschat, *Chem. Eur. J.* **2009**, 15, 2140–2147.
- [7] B. Wangler, G. Quandt, L. Iovkova, E. Schirrmacher, C. Wangler, G. Boening, M. Hacker, M. Schmoeckel, K. Jurkschat, P. Bartenstein, R. Schirrmacher, *Bioconjugate Chem.* **2009**, 20, 317–321.
- [8] W. J. McBride, R. M. Sharkey, H. Karacay, C. A. D'Souza, E. A. Rossi, P. Laverman, C.-H. Chang, O. C. Boerman, D. M. Goldenberg, *J. Nucl. Med.* **2009**, 50, 991–998.
- [9] W. J. McBride, C. A. D'Souza, R. M. Sharkey, H. Karacay, E. A. Rossi, C.-H. Chang, D. M. Goldenberg, *Bioconjugate Chem.* **2010**, 21, 1331–1340.
- [10] Y. Luo, *Handbook of Chemical Bond Energies*, CRC Press, Boca Raton, Florida, **2007**.
- [11] C. R. Wade, A. E. J. Broomsgrove, S. Aldridge, F. P. Gabbai, *Chem. Rev.* **2010**, 110, 3958–3984.
- [12] R. Ting, M. J. Adam, T. J. Ruth, D. M. Perrin, *J. Am. Chem. Soc.* **2005**, 127, 13094–13095.
- [13] D. M. Perrin, R. Ting, USA Pat. US2008/0038191, **2005**; *Chem. Abstr.* **2005**, 143, 253911.
- [14] E. Vedejs, R. W. Chapman, S. C. Fields, S. Lin, M. R. Schrimpf, *J. Org. Chem.* **1995**, 60, 3020–3027.
- [15] C. W. Harwig, R. Ting, M. J. Adam, T. J. Ruth, D. M. Perrin, *Tetrahedron Lett.* **2008**, 49, 3152–3156.
- [16] J. Culver, W. Akers, S. Achilefu, *J. Nucl. Med.* **2008**, 49, 169–172.
- [17] P. Agrawal, G. J. Strijkers, K. Nicolay, *Adv. Drug Delivery Rev.* **2010**, 62, 42–58.
- [18] K. R. Bhushan, P. Misra, F. Liu, S. Mathur, R. E. Lenkinski, J. V. Frangioni, *J. Am. Chem. Soc.* **2008**, 130, 17648–17649.
- [19] V. Ponomarev, M. Doubrovin, I. Serganova, J. Vider, A. Shavrin, T. Beresten, A. Ivanova, L. Ageyeva, V. Tourkova, J. Balatoni, W. Bornmann, R. Blasberg, J. Gelovani Tjuvajev, *Eur. J. Nucl. Med. Mol. Imaging* **2004**, 31, 740–751.
- [20] F. L. Thorp-Greenwood, M. P. Coogan, *Dalton Trans.* **2011**, 40, 6129–6143.
- [21] G. Ulrich, R. Ziessel, A. Harriman, *Angew. Chem.* **2008**, 120, 1202; *Angew. Chem. Int. Ed.* **2008**, 47, 1184–1201.
- [22] A. Loudet, K. Burgess, *Chem. Rev.* **2007**, 107, 4891–4932.
- [23] R. Ting, J. Lo, M. J. Adam, T. J. Ruth, D. M. Perrin, *J. Fluorine Chem.* **2008**, 129, 349–358.
- [24] T. W. Hudnall, T.-P. Lin, F. P. Gabbai, *J. Fluorine Chem.* **2010**, 131, 1182–1186.
- [25] Z. Li, T.-P. Lin, S. Liu, C.-W. Huang, T. W. Hudnall, F. P. Gabbai, P. S. Conti, *Chem. Commun.* **2011**, 47, 9324–9326.
- [26] D. Neri, C. T. Supuran, *Nat. Rev. Drug Discovery* **2011**, 10, 767–777.
- [27] G. L. Semenza, *Cancer Metastasis Rev.* **2007**, 26, 223–224.
- [28] C. C. Wykoff, N. J. P. Beasley, P. H. Watson, K. J. Turner, J. Pastorek, A. Sibtain, G. D. Wilson, H. Turley, K. L. Talks, P. H. Maxwell, C. W. Pugh, P. J. Ratcliffe, A. L. Harris, *Cancer Res.* **2000**, 60, 7075–7083.

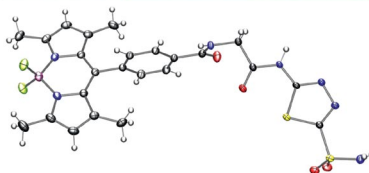
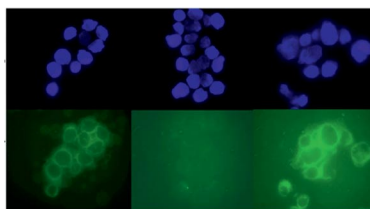
FULL PAPER

- [29] S. Parkkila, A.-K. Parkkila, J. Saarnio, J. Kivela, T. J. Karttunen, K. Kaunisto, A. Waheed, W. S. Sly, O. Tureci, I. Virtanen, H. Rajaniemi, *J. Histochem. Cytochem.* **2000**, *48*, 1601–1608.
- [30] J. A. Lancaster, A. L. Harris, S. E. Davidson, J. P. Logue, R. D. Hunter, C. C. Wyckoff, J. Pastorek, P. J. Ratcliffe, I. J. Stratford, C. M. L. West, *Cancer Res.* **2001**, *61*, 6394–6399.
- [31] S. K. Chia, C. C. Wyckoff, P. H. Watson, C. Han, R. D. Leek, J. Pastorek, K. C. Gatter, P. Ratcliffe, A. L. Harris, *J. Clin. Oncol.* **2001**, *19*, 3660–3668.
- [32] C. C. Wyckoff, N. Beasley, P. H. Watson, L. Campo, S. K. Chia, R. English, J. Pastorek, W. S. Sly, P. Ratcliffe, A. L. Harris, *Am. J. Pathol.* **2001**, *158*, 1011–1019.
- [33] J. Saarnio, S. Parkkila, A.-K. Parkkila, K. Haukipuro, S. Pastorekova, J. Pastorek, M. I. Kairaluoma, T. J. Karttunen, *Am. J. Pathol.* **1998**, *153*, 279–285.
- [34] A. Kivela, S. Parkkila, J. Saarnio, T. J. Karttunen, J. Kivela, A. K. Parkkila, A. Waheed, W. S. Sly, J. H. Grubb, G. Shah, O. Tureci, H. Rajaniemi, *Am. J. Pathol.* **2000**, *156*, 577–584.
- [35] K. J. Turner, J. P. Crew, C. C. Wyckoff, P. H. Watson, R. Poulson, J. Pastorek, P. J. Ratcliffe, D. Cranston, A. L. Harris, *Br. J. Cancer* **2002**, *86*, 1276–1282.
- [36] K. J. O'Byrne, G. Cox, D. Swinson, D. Richardson, J. G. Edwards, J. Lolljee, A. Andi, M. I. Koukourakis, A. Giatromanolaki, K. Gatter, A. L. Harris, D. Waller, J. L. Jones, *Lung Cancer* **2001**, *34* (Suppl. 2), S83–S89.
- [37] N. J. P. Beasley, C. C. Wyckoff, P. H. Watson, R. Leek, H. Turley, K. Gatter, J. Pastorek, G. J. Cox, P. Ratcliffe, A. L. Harris, *Cancer Res.* **2001**, *61*, 5262–5267.
- [38] D. Vullo, M. Franchi, E. Gallori, J. Pastorek, A. Scozzafava, S. Pastorekova, C. T. Supuran, *Bioorg. Med. Chem. Lett.* **2003**, *13*, 1005–1009.
- [39] O. Tureci, U. Sahin, E. Vollmar, S. Siemer, E. Gottert, G. Seitz, A.-K. Parkkila, G. N. Shah, J. H. Grubb, M. Pfreundschuh, W. S. Sly, *Proc. Natl. Acad. Sci. USA* **1998**, *95*, 7608–7613.
- [40] J.-Y. Winum, D. Vullo, A. Casini, J.-L. Montero, A. Scozzafava, C. T. Supuran, *J. Med. Chem.* **2003**, *46*, 2197–2204.
- [41] J.-Y. Winum, D. Vullo, A. Casini, J.-L. Montero, A. Scozzafava, C. T. Supuran, *J. Med. Chem.* **2003**, *46*, 5471–5477.
- [42] C. T. Supuran, *Nat. Rev. Drug Discovery* **2008**, *7*, 168–181.
- [43] S. Pastorekova, A. Casini, A. Scozzafava, D. Vullo, J. Pastorek, C. T. Supuran, *Bioorg. Med. Chem. Lett.* **2004**, *14*, 869–873.
- [44] D. Vullo, A. Innocenti, I. Nishimori, J. Pastorek, A. Scozzafava, S. Pastorekova, C. T. Supuran, *Bioorg. Med. Chem. Lett.* **2005**, *15*, 963–969.
- [45] V. Alterio, R. M. Vitale, S. M. Monti, C. Pedone, A. Scozzafava, A. Cecchi, G. De Simone, C. T. Supuran, *J. Am. Chem. Soc.* **2006**, *128*, 8329–8335.
- [46] T. Tsuji, K. Gonda, Y. Aoyama, T. Tokunaga, S. Sando, *Chem. Lett.* **2011**, *40*, 1275–1277.
- [47] K. D. Brubaker, F. Mao, C. V. Gay, *J. Histochem. Cytochem.* **1999**, *47*, 545–550.
- [48] C. T. Supuran, A. Scozzafava, A. Casini, *Med. Res. Rev.* **2003**, *23*, 146–189.
- [49] D. Le Bars, S. K. Luthra, V. W. Pike, E. R. Swenson, *Appl. Radiat. Isot.* **1988**, *39*, 671–675.
- [50] M. Rami, J.-Y. Winum, A. Innocenti, J.-L. Montero, A. Scozzafava, C. T. Supuran, *Bioorg. Med. Chem. Lett.* **2008**, *18*, 836–841.
- [51] C. T. Supuran, G. Manole, M. Andruh, *J. Inorg. Biochem.* **1993**, *49*, 97–103.
- [52] C. T. Supuran, *Met.-Based Drugs* **1995**, *2*, 331–336.
- [53] A. Cecchi, A. Hulikova, J. Pastorek, S. Pastorekova, A. Scozzafava, J.-Y. Winum, J.-L. Montero, C. T. Supuran, *J. Med. Chem.* **2005**, *48*, 4834–4841.
- [54] M. Rami, A. Maresca, F.-Z. Smaine, J.-L. Montero, A. Scozzafava, J.-Y. Winum, C. T. Supuran, *Bioorg. Med. Chem. Lett.* **2011**, *21*, 2975–2979.
- [55] A. Cui, X. Peng, J. Fan, X. Chen, Y. Wu, B. Guo, *J. Photochem. Photobiol. A: Chem.* **2007**, *186*, 85–92.
- [56] A. M. Grant, S. V. Krees, A. B. Mauger, W. J. Rzeszotarski, F. W. Wolff, *J. Med. Chem.* **1972**, *15*, 1082–1084.
- [57] J. H. Brannon, D. Magde, *J. Phys. Chem.* **1978**, *82*, 705–709.
- [58] Y. Chen, J. Jiang, *Acta Crystallogr., Sect. E Struct. Rep. Online* **2011**, *67*, o908.
- [59] X. Yin, Y. Li, Y. Zhu, X. Jing, Y. Li, D. Zhu, *Dalton Trans.* **2010**, *39*, 9929–9935.
- [60] Q. Zheng, G. Xu, P. N. Prasad, *Chem. Eur. J.* **2008**, *14*, 5812–5819.
- [61] P. Vandersluis, A. L. Spek, *Acta Crystallogr., Sect. A* **1990**, *46*, 194–201.
- [62] A. L. Spek, *J. Appl. Crystallogr.* **2003**, *36*, 7–13.
- [63] A. L. Spek, PLATON/SQUEEZE, Utrecht, The Netherlands, **1998**.
- [64] P. A. Waghorn, DPhil Thesis, Oxford, **2011**.
- [65] C. V. Gay, W. J. Mueller, *Science* **1974**, *183*, 432–434.
- [66] C. V. Gay, E. J. Faleski, H. Schraer, R. Schraer, *J. Histochem. Cytochem.* **1974**, *22*, 819–825.
- [67] H. E. Gottlieb, V. Kotlyar, A. Nudelman, *J. Org. Chem.* **1997**, *62*, 7512–7515.
- [68] J. Cosier, A. M. Glazer, *J. Appl. Crystallogr.* **1986**, *19*, 105–107.
- [69] Z. Otwinowski, W. Minor, *Macromol. Crystallogr., Part A* **1997**, *276*, 307–326.
- [70] A. Altomare, G. Casciarano, C. Giacovazzo, A. Guagliardi, *J. Appl. Crystallogr.* **1994**, *27*, 1045–1050.
- [71] D. Watkin, R. Cooper, C. K. Prout, *Z. Kristallogr.* **2002**, *217*, 429–430.
- [72] Graphpad Software, San Diego, CA, USA, www.graphpad.com.

Received: December 8, 2011

Published Online: ■

4,4-Difluoro-4-borata-3a-azonia-4a-aza-*s*-indacene (BODIPY)-functionalised sulfonamides have been tested for their carbonic anhydrase (CA) selectivity by binding-affinity assays against CA IX and CA XII. In vitro studies in a CA IX transfected cell line have highlighted the importance of both the nature of the fluorophore and the presence of a secondary binding interaction for selective CA inhibition.



**P. A. Waghorn,* M. W. Jones,
A. McIntyre, A. Innocenti, D. Vullo,
A. L. Harris, C. T. Supuran,
J. R. Dilworth 1–11**

Targeting Carbonic Anhydrases with
Fluorescent BODIPY-Labelled Sulfon-
amides

Keywords: Carbonic anhydrases / Sulfon-
amides / Fluorescence / BODIPY / Imaging
agents